A dual photobase system for directing the pathway of pH-sensitive chemical reactions with light

Anna Yucknovsky and Nadav Amdursky*

Schulich Faculty of Chemistry, Technion - Israel Institute of Technology, Haifa 3200003, Israel

*Corresponding author e-mail: amdursky@technion.ac.il

Abstract

Light-gated chemical reactions allow spatial and temporal control of chemical processes. Here, we suggest a new system for controlling pH-sensitive processes with light using two photobases of Arrhenius and Brønsted types. Only after light excitation do Arrhenius photobases undergo hydroxide ion dissociation, while Brønsted photobases capture a proton. However, none can be used alone to reversibly control pH due to the limitations arising from excessively fast or overly slow photoreaction timescales. We show here that combining the two types of photobases allows light-triggered and reversible pH control. We show an application of this method in directing the pH-dependent reaction pathways of the organic dye Alizarin Red S simply by switching between different wavelengths of light, i.e., irradiating each photobase separately. The concept of a light-controlled system shown here of a sophisticated interplay between two photobases can be integrated into various smart functional and dynamic systems.

Keywords: Photobases, Photochemistry, Dynamic networks, Alizarin Red S, 6-Methoxyquinoline, Malachite green carbinol base

Introduction

Light-controlled chemical reactions have been established as a tool to achieve spatial and temporal control over chemical processes, making it possible to localize reactions or develop complex chemical networks. This tool can also be used for the regulation of biological processes, the development of smart materials, and the understanding of the complexity of nature.[1-5] In light-controlled chemical reactions, light acts as an external stimulus on the gate, a substance that undergoes a certain photoreaction, providing remote control over the desired chemical process. To date, most photoswitches, such as azobenzene, spiropyran, and their derivatives, have been used to gate the reactions.[6-16] In this work, we use a different type of photoresponsive molecule called a photobase of two different categories. Brønsted photobases are compounds that are weak bases in their ground state; however, they become strong bases capable of proton capture in their electronically excited state.[17-21] Several molecules have shown the capability to serve as a Brønsted photobase, consisting of mainly quinoline-based and acridine-based molecules, although several other molecules have shown this capability.[22-27] Arrhenius photobases are capable of hydroxide ion release in their electronically excited state. The most notable example of a reversible Arrhenius photobase is malachite green carbinol base (MGCB) and its water-soluble methylated derivative.[28-31] Brønsted photobases have been used to control chemical reactions in various functional systems, including catalysis photoactivation, light-induced droplet self-propulsion, photocurrent generation, dynamic self-assembly, and light-modulated ionic transport.[32-35] The use of MGCB in functional systems involves light-driven DNA conformational switches, photoresponsive hydrogels, dynamic self-assembly, and photoresponsive photonic crystals.[36-39]

In this work, we control the reaction pathways of the organic dye Alizarin Red S (ARS) using the unique interaction between two photobases of Arrhenius and Brønsted types, having different excitation wavelengths and photoreaction timescales. We show that by a sophisticated interplay between them, we can use the advantages and compensate for the disadvantages of each of them. Namely, an Arrhenius photobase can raise the pH of a solution after excitation because of its very slow recombination with hydroxide; however, this can become a disadvantage when the pH needs to be reversibly controlled. A Brønsted photobase can instantaneously and reversibly capture a proton from water upon excitation; however, due to the rapid reversibility of proton transfer, the change in the pH of the solution is temporal on the nanosecond timescale. By combining both types of photobases, we succeeded in changing the pH reversibly on a second to minute timescale. Thus, the pH increased due to the excitation of the Arrhenius photobase and the subsequent release of the hydroxide and then decreased by

speeding the rate of the reaction toward recombination by increasing the concentration of the product (hydroxide), facilitated by the excitation of the Brønsted photobase. Here, we use our new approach for pH control, which results in directing the reaction pathways of ARS. ARS is known to undergo different reactions, either with phenylboronic acid (PBA) or Ni(II), which are pH-sensitive and can be monitored using spectroscopy.[40-42] Since the two reactions have an opposite pH response, we could direct ARS toward each pathway using our system of two photobases. Altogether, the new concepts we introduce here can be used both for the fundamental understanding of the mechanism of photobases as well as their utilization in various systems.

Results and Discussion

In the first part, we studied the interplay between the two photobases, Arrhenius and Brønsted. We used MGCB and 6-methoxyquinoline (6MQ) as the Arrhenius and Brønsted photobases, respectively. One of the hallmarks of both photobases is the different electronic structures before and after hydroxide release for MGCB and protonation for 6MQ. We used UV–Vis absorption to follow the different electronic structures of MGCB and 6MQ (**Figures 1a** and **1b**, respectively). MGCB in its neutral form has absorption bands in the UV range, but after hydroxide release, in its cationic form, it has an intense absorption band at 620 nm (**Figure 1a**). The rapid release of hydroxide from MGCB is due to a sharp change in the dissociation constant of the molecule (i.e., hydroxide release) when excited at ~300 nm.[29] However, the reverse reaction, i.e., the recombination of the MGCB cation with the hydroxide, proceeds very slowly on the timescale of hours.[43-45] To solve this problem, we introduce here a method to accelerate MGCB recombination by adding a 6MQ photobase (**Figure 1b**). When exciting (at 330 nm) unprotonated 6MQ in an aqueous environment, its pK_a jumps from 5.18 to 11.8, resulting in protonation and proton abstraction from water (or another available proton donor). Unlike MGCB, proton capture by 6MQ and its re-dissociation are fast with nanosecond timescales.[21] Although the excitation of 6MQ results in hydroxide formation, it does not result in a pH jump due to the ultrafast proton dissociation as 6MQ returns to its ground state.

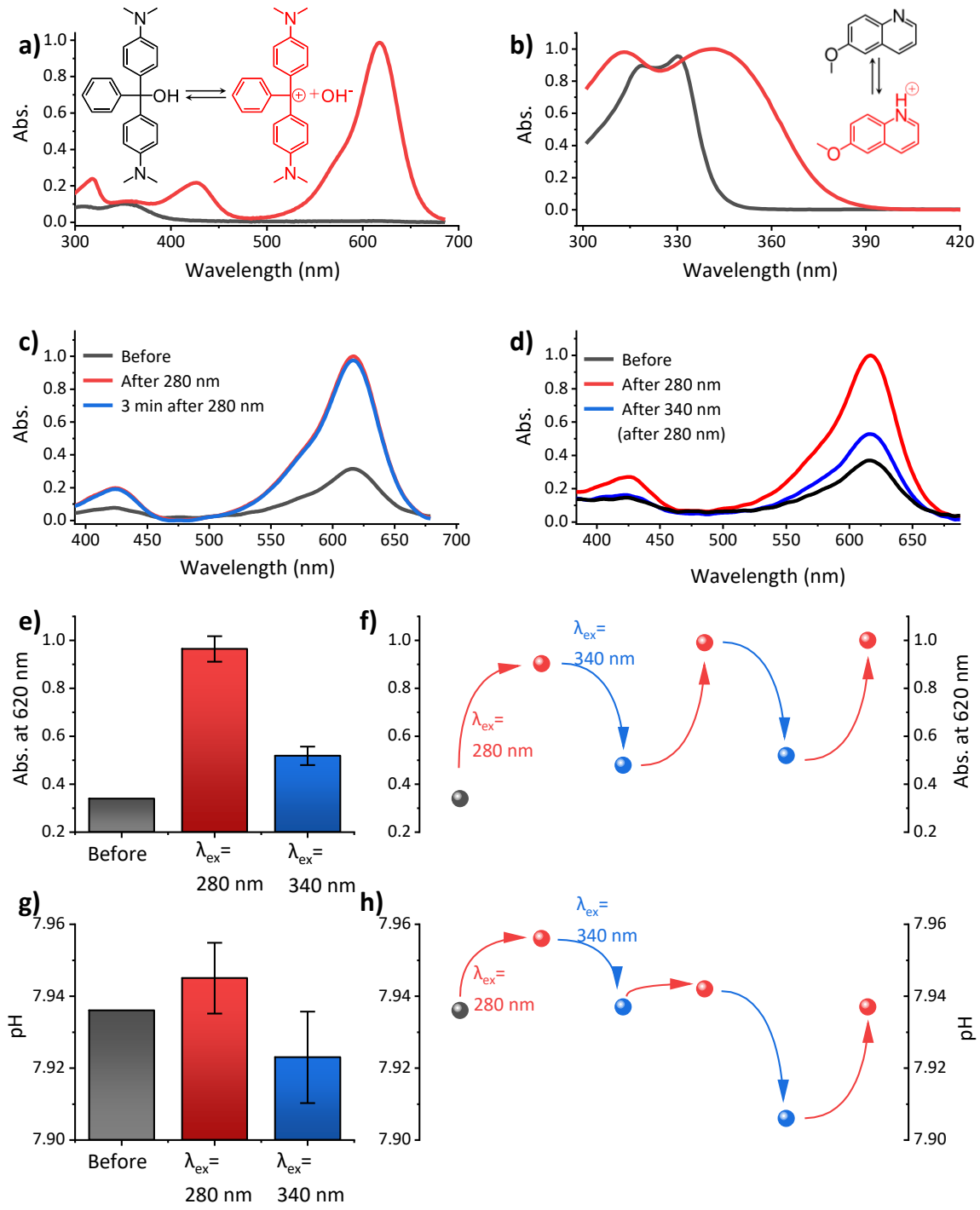

Figure 1. The interaction between MGCB and 6MQ photobases. Normalized absorption spectra of **a)** MGCB in alkaline (black curve) and acidic (red curve) conditions and **b)** 6MQ in neutral (black curve) and acidic (red curve) conditions, together with their structure and photochemical process. **c)** Normalized absorption spectra of MGCB solution (at slightly basic conditions) before, immediately after, and 3 min after 280 nm excitation. **d)** Normalized absorption spectra of a solution containing both MGCB and 6MQ before irradiation, after 280 nm excitation, and after 340 nm excitation. **e)** Changes in the absorption intensity (at 620 nm) and **g)** in the pH of a solution containing MGCB and 6MQ following excitation at 280 nm and the subsequent excitation at 340 nm, together with a representative cycle of the change in **f)** the absorption and **h)** the pH upon alternating excitations at 280 and 340 nm.

In our work, we hypothesize that when 6MQ is added to MGCB, the pH of the solution can be changed reversibly because 6MQ can affect the recombination rate of MGCB. To follow the state of MGCB with and without the addition of 6MQ, we acquired the visible absorption (6MQ does not absorb in the visible region, **Figure 1b**) before, immediately after 280 nm excitation, and a few minutes after excitation (**Figure 1c** and **1d** for without and with the addition of 6MQ, respectively). In both cases, the results show an immediate appearance of an intense absorption band at 620 nm after excitation, indicating the formation of the MGCB cation. In the absence of 6MQ, there was no significant change in intensity in the subsequent measurement due to the slow hydroxide recombination rate (**Figure 1c**). However, in the presence of 6MQ, where we also used an additional 340 nm excitation to excite 6MQ after the irradiation of MGCB at 280 nm, the intensity of the cationic MGCB band dropped considerably, indicating the recombination of the MGCB cation with the hydroxide anion (**Figure 1d**). As a control experiment, we replaced the 6MQ photobase with a 2-naphthol-6-sulfonate (2N6S) Brønsted photoacid and repeated the experiment **(Figure S1**). A photoacid is a molecule that acts in a reverse manner to a Brønsted photobase, i.e., upon excitation with light, its pK_a drops sharply, leading to proton release.[46] The results indicate no changes in the intensity of the 620 nm band upon excitation with 2N6S, which confirms our assumption that 6MQ affects the rate of MGCB recombination.

An important requirement for the design of any dynamic system is the capability to control the system in a reversible manner. Accordingly, in the next step, we followed the reversibility of the interaction between the photobases. To do so, we traced the changes in the absorption intensity of the MGCB cation (at 620 nm) in a solution containing both MGCB and 6MQ photobases following excitation at 280 nm and subsequent excitation at 340 nm (**Figure 1e**). As shown in the figure, upon excitation of MGCB (at 280 nm) and 6MQ (at 340 nm), the absorbance at 620 nm rises and falls, respectively, which can be repeated over several cycles (**Figure 1f** and **Figure S2** for the full spectra). These results show that our dual photobase system provides reversible hydroxide release, i.e., light-controlled pH change. Consequently, we followed the pH of the solution containing MGCB and 6MQ photobases following excitation at 280 nm and subsequent excitation at 340 nm (**Figure 1g**). Additionally, the change in the pH shows a similar pattern, i.e., a pH increase upon the excitation of MGCB (at 280 nm), associated with hydroxide release, and a pH drop upon the excitation of 6MQ (at 340 nm), associated with hydroxide recombination, which can be repeated over several cycles (**Figure 1h**).

Next, we turned to kinetics measurements to understand the interaction mechanism between the MGCB and 6MQ photobases. To do so, we followed the transient change in MGCB absorption (at 620 nm), which is indicative of its dissociation and recombination, with or without the addition of 6MQ (**Figure 2**). Regardless of the presence of 6MQ, upon a short (2 sec) irradiation pulse at 280 nm, we observed a rapid increase in the absorbance, indicative of hydroxide dissociation from MGCB, that immediately stopped when the irradiation stopped. As stated, the recombination process of MGCB is slow, and from the transient measurement, we calculated the slow decay time scale to be 1620±255 sec (**Figure 2a**). However, when 6MQ was present in the solution and upon an additional irradiation pulse (20 sec) at 340 nm that excites 6MQ, we observed a significantly faster decay of the MGCB absorption with a time scale of 156±36 sec (**Figure 2b** and **Figure S3** for repeated cycles), i.e., a faster MGCB recombination. It should be noted that the main change in the decay was observed only after 340 nm irradiation and not during irradiation, where we observed only a slight decrease in intensity. To understand the difference between the processes occurring during and after the irradiation of 6MQ at 340 nm, we followed the absorption (at 620 nm) kinetics of the solution containing only MGCB under irradiation at 340 nm (**Figure S4**), i.e., without the 280 nm irradiation in the beginning. We noticed that in this condition, 340 nm irradiation resulted in an increase in the absorption intensity at 620 nm, meaning that MGCB is also excited to some extent at this light wavelength. It is noteworthy that the fraction of MGCB molecules excited using 340 nm irradiation is negligible compared to 280 nm irradiation. Indeed, while following the kinetics of the solution containing only MGCB upon irradiation pulses of both 280 and 340 nm (**Figure S5**), we can observe that the decay stops during 340 nm irradiation. Based on this finding, we suggest that in the measurement presented in **Figure 2b,** the slower recombination decay observed during irradiation at 340 nm (compared to the dark) is due to a minor contribution of excited MGCB.

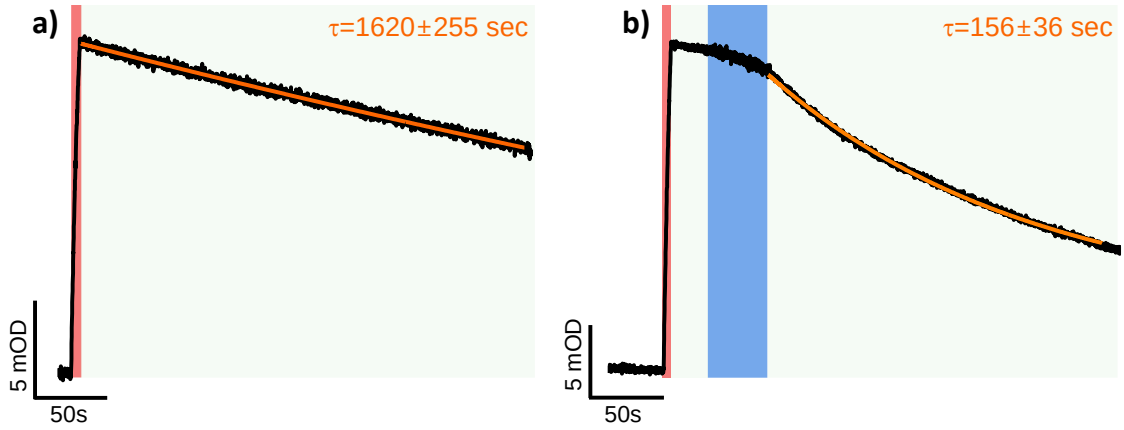

Figure 2. Kinetics measurements. The absorption intensity at 620 nm of the MGCB solution (**a**) without and (**b**) with 6MQ in the solution upon irradiation at 280 nm (red) and in (b) upon subsequent irradiation at 340 nm (blue).

Following the experimental validation that the excitation of 6MQ can result in the enhancement of the recombination rate of MGCB, we propose the following mechanism to address how 6MQ accelerates MGCB recombination during excitation and in the dark (**Scheme 1**). 1) When excited at 280 nm, MGCB releases hydroxide to form the MGCB cation. 2) The MGCB cation has three resonance structures, among which the carbocation structure (in the middle) is the only one suitable for recombination with hydroxide. However, this structure is unstable, and the positive charge is delocalized. 3) The solution contains an excess of 6MQ molecules relative to MGCB, some of which are located near the MGCB carbocation. When excited at 340 nm, 6MQ abstracts protons from water, increasing the hydroxide concentration near the MGCB carbocation. 4) An excess of hydroxide next to the MGCB carbocation increases its stability since it causes a change in the hybridization of the central carbon and a subsequent increase in the density of the positive charge on it, activating the MGCB-hydroxide pair.[44-45] 5) The activated pair of MGCB carbocation-hydroxide recombines.

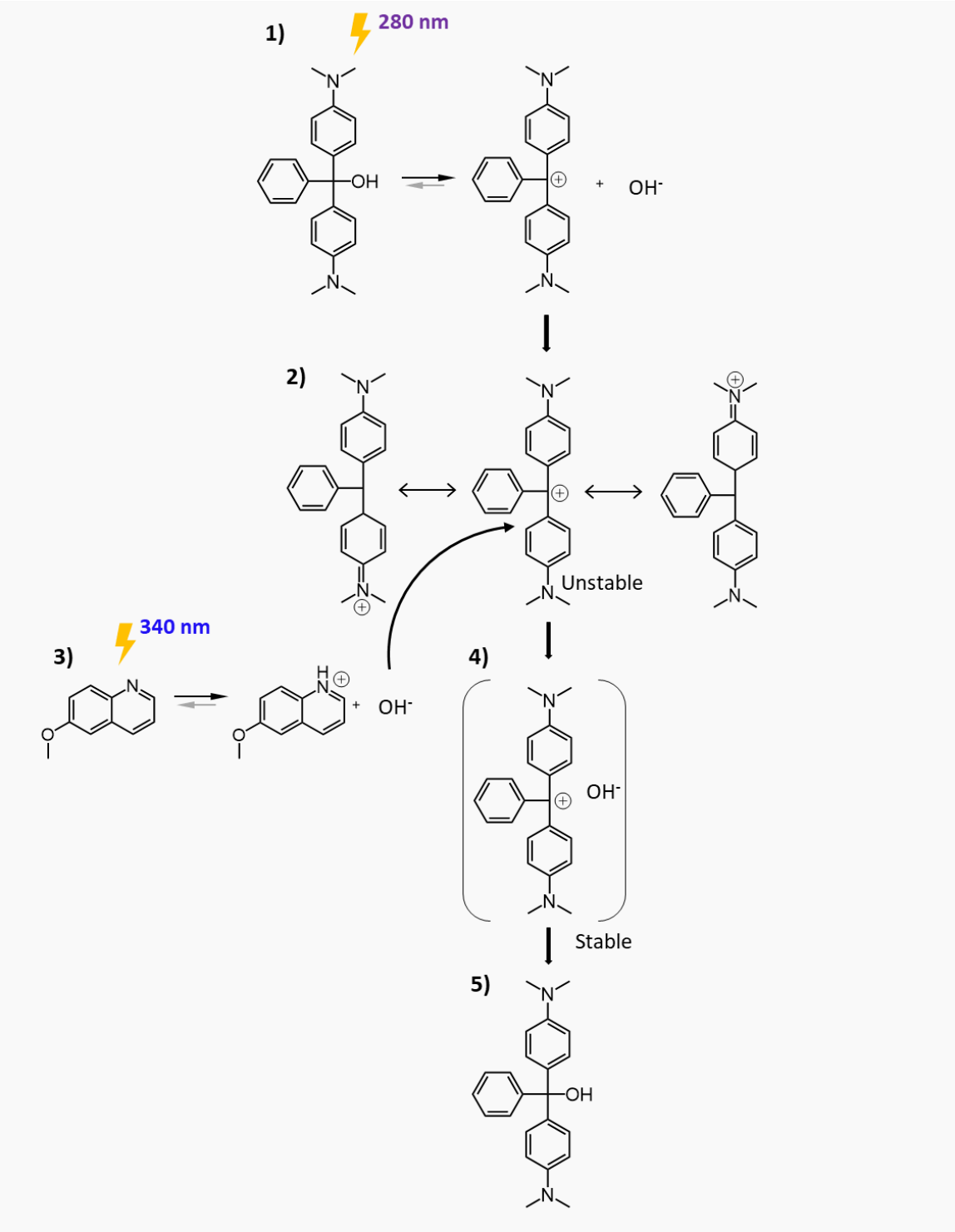

Scheme 1. The mechanism of MGCB and 6MQ interaction.

One of the interesting outcomes of our results is the ability of 6MQ, being a Brønsted photobase only during its short excited state lifetime, to enhance the recombination rate of the MGCB photobase on the seconds to minutes time scales after excitation. This can be possible only due to our suggested increase in the hydroxide concentration near the MGCB carbocation that interacts with the latter, thus preventing the recombination of the hydroxide with 6MQ upon its return to its ground state. To validate this hypothesis, we explored how the 340 nm light duration, i.e., the time of excitation of 6MQ, influences the recombination time scales of

MGCB (**Table S1**). According to our suggestion, the increase in the 340 nm light duration will increase the available hydroxide concentration for the interaction with the MGCB carbocation, thus resulting in faster MGCB recombination, which is what we observe in Table S1.

Based on the results of the first part, in the second part of the study, we used our dual photobase system, enabling the manipulation of pH, to direct the reactions of Alizarin Red S (ARS). ARS can form a complex with phenylboronic acid (PBA)[40, 47] or Ni(II)[42] (**Scheme 2**). Both reactions are fast and can be monitored by spectroscopy owing to the characteristic emission band at 580 nm of the ARS-PBA complex (**Figure S6**) and the characteristic absorption band at 540 nm of the ARS-Ni (non-emitting) complex (**Figure S7**). It is important to note that the calculated equilibrium constants of the ARS-PBA and ARS-Ni complex formation reactions, 2.9×10^3 and 21.8×10^3, respectively (**Figures S8** and **S9** for the calculations), show an order of magnitude difference; thus, we used an excess of PBA in the experiments described below.

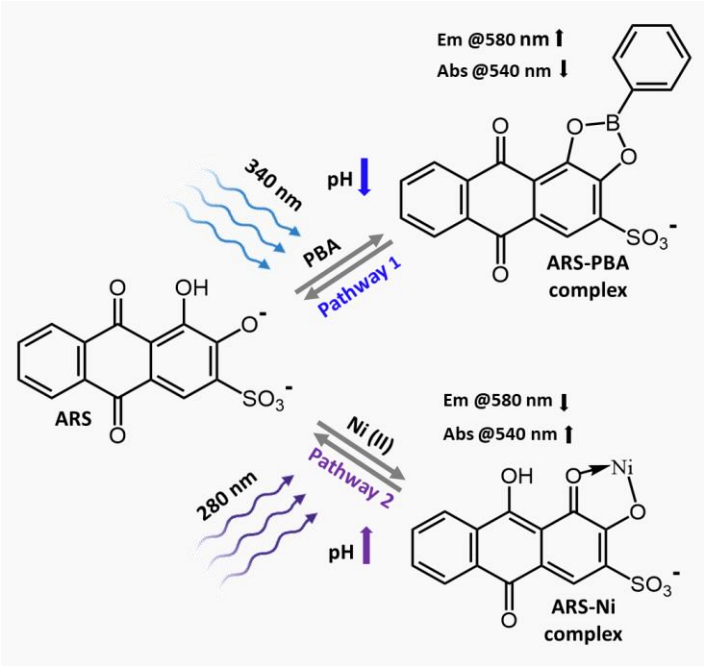

Scheme 2. Reaction pathways of ARS. Molecular schemes of ARS and the products of the reaction with PBA or Ni(II). In pathway 1, when irradiated at 340 nm, the reaction with PBA is preferable, as indicated by a decrease in the absorption intensity at 540 nm along with an increase in the emission intensity at 580 nm (Figure 3). In pathway 2, when irradiated at 280 nm, the reaction with Ni(II) is preferable, as indicated by an increase in the absorption intensity at 540 nm along with a decrease in the emission intensity at 580 nm (Figure 3).

To verify our hypothesis that changes in the pH of the solution will influence the reaction pathway of ARS, we first followed the spectrophotometric pH titration of each reaction mixture individually, one with ARS and PBA and the other with ARS and Ni(II). We observed that the emission intensity of ARS-PBA (**Figure 3a**) and the absorption intensity of the ARS-Ni complexes (**Figure 3b**) decrease and increase, respectively, with increasing pH, thus indicating

the destruction of ARS-PBA and the formation of ARS-Ni with increasing pH. Unlike the emission of the ARS-PBA complex, its absorption is less sensitive to changes in pH, showing a red shift with increasing pH (**Figure S10**).

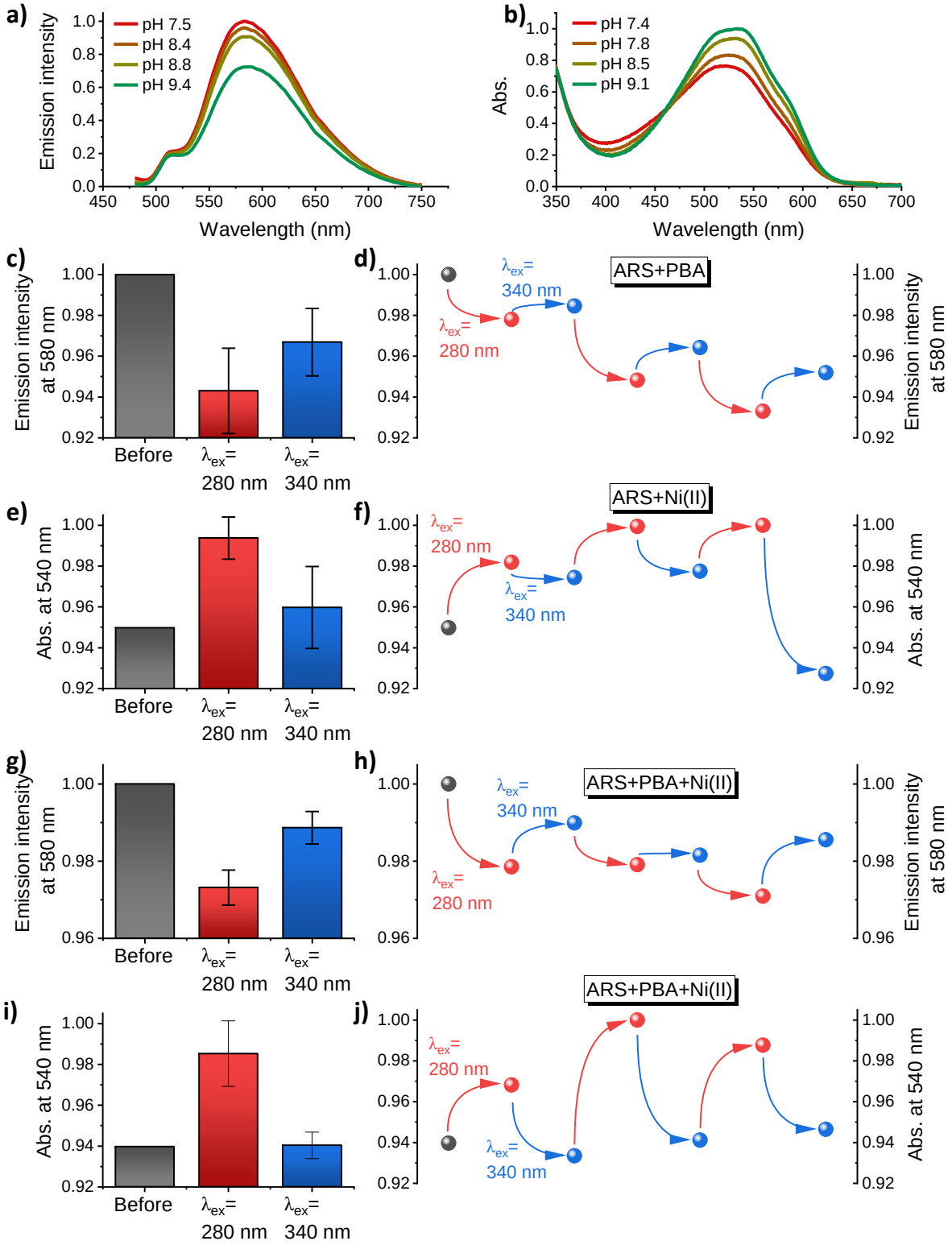

Figure 3. Controlling reaction pathways of ARS. a) and **b)** Normalized emission and absorption spectra of ARS-PBA and ARS-Ni complexes, respectively, upon pH titration. **c)** Changes in the emission intensity (at 580 nm) of a solution containing ARS, PBA, MGCB, and 6MQ following excitation at 280 nm and subsequent excitation at 340 nm, together with **d)** a

representative cycle of the change in the emission upon alternating excitation at 280 and 340 nm. **e)** Changes in the absorption intensity (at 540 nm) of a solution containing ARS, Ni(II), MGCB, and 6MQ following excitation at 280 nm and subsequent excitation at 340 nm, together with **f)** A representative cycle of the change in the absorption upon alternating excitation at 280 and 340 nm. **g)** and **i)** Changes in the emission intensity (at 580 nm) and absorption intensity (at 540 nm), respectively, of a solution containing ARS, PBA, Ni(II), MGCB, and 6MQ following excitation at 280 nm and the subsequent excitation at 340 nm, together with a representative cycle of the change in **h)** the emission and **j)** the absorption upon alternating excitations at 280 and 340 nm.

In the next step, we tested the capability of our new MGCB – 6MQ system to control the reaction of ARS either with PBA or with Ni ions. To do so, we prepared two mixtures: 1) ARS with PBA, MGCB, and 6MQ and 2) ARS with Ni(II), MGCB, and 6MQ. We subjected both mixtures to alternating excitation at 280 and 340 nm and monitored the emission (at 580 nm) and the absorption (at 540 nm) of the ARS-PBA and ARS-Ni complexes, respectively (**Figures 3c-3f** and **S11-S12** presenting the full spectra). The results show that exciting MGCB (at 280 nm) has a destructive and constructive effect on the formation of ARS-PBA and ARS-Ni complexes, respectively, in the two different solutions. In comparison, exciting 6MQ (at 340 nm) has the opposite effect on the complexes in the two solutions. Notably, the reversible increase and decrease in the concentration of each of the complexes could be repeated for several irradiation cycles. To provide additional support for reversibility, we followed the absorption of the ARS-Ni complex at 540 nm using kinetics measurements (**Figure S13**) (unfortunately, it is not possible to conduct kinetic fluorescence measurements during different excitations). We observed a steep increase in absorption during 280 nm irradiation that was stopped in the dark, indicating the formation of ARS-Ni. Subsequently, we observed a steep drop in absorption during 340 nm irradiation, followed by a more moderate decrease in the dark, both associated with the destruction of the ARS-Ni complex. The decay time scales measured in the dark were consistent with those measured for the solution of MGCB and 6MQ (**Figure 2b**).

Last, we controlled the two different ARS reactions with PBA or Ni(II) and direct ARS in two possible pathways, with both PBA and Ni(II) present in the same reaction mixture. We prepared a solution containing all the different components (ARS, PBA, Ni(II), MGCB, and 6MQ) and followed both the emission and absorption under alternating 280 and 340 nm excitation (**Figures 3g-3j**, the full spectra are shown in **Figures S14** and **S15**). As discussed, because of the different equilibrium constants of ARS-PBA and ARS-Ni complexes, we used an excess of PBA (see experimental). We found that the ARS reaction is directed to form the ARS-Ni complex when exciting MGCB (at 280 nm), as indicated by an increase in the absorption

intensity of ARS-Ni along with a decrease in the emission intensity of ARS-PBA. However, when exciting 6MQ (at 340 nm), the ARS reaction occurs in a different direction, favoring the formation of the ARS-PBA complex, as indicated by an increase in the ARS-PBA emission intensity along with a decrease in the ARS-Ni absorption intensity. As before, the change in the reaction pathway is reversible, as indicated by several irradiation cycles. The two pathways are summarized in **Scheme 2**, whereas the formation of one complex occurs at the expense of the other (and *vice versa*).

Conclusion

In summary, we have developed here a system of two photobases of different types - Arrhenius and Brønsted. By combining both types of photobases, represented by MGCB and 6MQ, it was possible to adjust the pH by exciting them, each with a suitable wavelength. The governing mechanism for the use of two different photobases is a tandem mechanism, starting by light-triggering hydroxide release from MGCB, thus forming an MGCB carbocation, followed by the excitation of 6MQ, resulting in protonation and the transient formation of hydroxide ions in solution. The excitation of 6MQ promotes the recombination of the MGCB carbocation with a hydroxide ion to reform the neutral MGCB. Accordingly, we suggest that this recombination of MGCB is a stepwise process within which MGCB-hydroxide pair activation must occur before the final recombination. We showed the applicability of the two-photobase system to control the reaction pathway of ARS. Using a solution that contained MGCB, 6MQ, ARS, and the two components of the different pathways, Ni ions and PBA, we showed that ARS can be directed to react either with Ni(II) or PBA by switching between 280 and 340 nm irradiation, which is associated with MGCB and 6MQ excitation, respectively. We followed the reactions of ARS with Ni(II) and PBA by measuring the former's absorption and the latter's emission and showed that upon excitation of the MGCB photobase, the ARS-Ni complex was formed at the expense of ARS-PBA, and upon excitation of the 6MQ photobase, the reverse trend was observed, i.e., the formation of the ARS-PBA complex at the expense of ARS-Ni. Our new double-photobase system to modulate pH-responsive chemical reactions can be useful for light-triggering various systems and can be incorporated into functional synthetic or biological materials.

Acknowledgments

A.Y. is supported by the Ariane de Rothschild Fellowship. N.A. thanks the US-Israel Binational Science Foundation (number 2018239) and the Ministry of Science and Technology (number 3-16243) for financial support.

Experimental Section

Chemicals: Malachite Green Carbinol base (MGCB) (Glentham Life Sciences), 6-methoxyquinoline (6MQ) (Alfa Aesar), Alizarin Red S (ARS) (Apollo Scientific), phenylboronic acid (PBA) (Chem-Impex International), and $NiCl_2 \cdot 6H_2O$ (Alfa Aesar) were used.

Solution preparation: The following stock solutions were prepared: [MGCB]=10 mM in EtOH, [$NiCl_2 \cdot 6H_2O$]=6 mM in water, [PBA]=0.1 M in EtOH, [6MQ]=0.5 M in EtOH, and [ARS]=7 mM in water. The final concentrations used in water (pH~7.5) were [MGCB]=0.01 mM, [6MQ]=0.5 mM, [ARS]=0.02 mM, [PBA]=0.2 mM, and [$NiCl_2$]=0.006 mM. Only for MGCB solutions was the 0.01 mM solution in water left overnight, in which the color of the solution changed from light blue (indicating the presence of the MGCB cation) to colorless (the neutral form). For alkaline and acidic solutions, NaOH and HCl were added to the aqueous solution.

UV–Vis and fluorescence measurements: UV–Vis measurements were performed using a Cary 60 spectrophotometer (Agilent), and fluorescence measurements were performed using a Fluorolog fluorometer (HORIBA). A 0.5 x 1.0 cm quartz cuvette was used. For UV–Vis kinetic measurements, a custom-built setup to connect LED light sources to a cuvette holder was used.

Light sources: 340 nm LED (130 mW) and 285 nm LED (40 mW) (both from SETi) were used.

References

(1) Liu, J.; Butt, H. J.; Wu, S., Reconfigurable surfaces based on photocontrolled dynamic bonds. *Adv. Funct. Mater.* **2020,** *30* (26), 1907605.
(2) Hoorens, M. W.; Szymanski, W., Reversible, spatial and temporal control over protein activity using light. *Trends Biochem. Sci* **2018,** *43* (8), 567-575.
(3) Göstl, R.; Senf, A.; Hecht, S., Remote-controlling chemical reactions by light: toward chemistry with high spatiotemporal resolution. *Chem. Soc. Rev.* **2014,** *43* (6), 1982-1996.
(4) Lee, J., Light-Controlled Chemical Reactions and Their Applications in Biological Systems. *Asian J. Org. Chem.* **2014,** *3* (8), 830-837.
(5) Peiris, E.; Hanauer, S.; Le, T.; Wang, J.; Salavati-fard, T.; Brasseur, P.; Formo, E. V.; Wang, B.; Camargo, P. H., Controlling Selectivity in Plasmonic Catalysis: Switching Reaction Pathway from Hydrogenation to Homocoupling Under Visible-Light Irradiation. *Angew. Chem. Int. Edit.* **2023,** *62* (4), e202216398.

(6) Klajn, R., Spiropyran-based dynamic materials. *Chem. Soc. Rev.* **2014,** *43* (1), 148-184.
(7) Keyvan Rad, J.; Balzade, Z.; Mahdavian, A. R., Spiropyran-based advanced photoswitchable materials: A fascinating pathway to the future stimuli-responsive devices. *J. Photochem. Photobiol., C* **2022,** *51*, 100487.
(8) Kumar, A.; Sahoo, P. R.; Prakash, K.; Arya, Y.; Kumar, S., Light controlled dimerization of spiropyran as a tool to achieve dual responsive capture and release system in aqueous media. *J. Electroanal. Chem.* **2021,** *903*, 115845.
(9) Hammarson, M.; Andersson, J.; Li, S.; Lincoln, P.; Andréasson, J., Molecular AND-logic for dually controlled activation of a DNA-binding spiropyran. *Chem. Commun.* **2010,** *46* (38), 7130-7132.
(10) Del Canto, E.; Natali, M.; Movia, D.; Giordani, S., Photo-controlled release of zinc metal ions by spiropyran receptors anchored to single-walled carbon nanotubes. *Phys. Chem. Chem. Phys.* **2012,** *14* (17), 6034-6043.
(11) Leippe, P.; Frank, J. A., Designing azobenzene-based tools for controlling neurotransmission. *Curr. Opin. Struct. Biol.* **2019,** *57*, 23-30.
(12) Liu, R.; Zhang, X.; Xia, F.; Dai, Y., Azobenzene-based photoswitchable catalysts: State of the art and perspectives. *J. Catal.* **2022,** *409*, 33-40.
(13) Cheng, H. B.; Zhang, S.; Qi, J.; Liang, X. J.; Yoon, J., Advances in application of azobenzene as a trigger in biomedicine: Molecular design and spontaneous assembly. *Adv. Mater.* **2021,** *33* (26), 2007290.
(14) Kume, S.; Murata, M.; Ozeki, T.; Nishihara, H., Reversible photoelectronic signal conversion based on photoisomerization-controlled coordination change of azobenzene-bipyridine ligands to copper. *J. Am. Chem. Soc.* **2005,** *127* (2), 490-491.
(15) Fu, W.; Pi, Y.; Gao, M.; Wang, W.; Li, C.; Tan, R.; Yin, D., Light-controlled cooperative catalysis of asymmetric sulfoxidation based on azobenzene-bridged chiral salen Ti IV catalysts. *Chem. Commun.* **2020,** *56* (44), 5993-5996.
(16) Stricker, F.; Sanchez, D. M.; Raucci, U.; Dolinski, N. D.; Zayas, M. S.; Meisner, J.; Hawker, C. J.; Martínez, T. J.; Read de Alaniz, J., A multistage single photochrome system for controlled photoswitching responses. *Nat. Chem.* **2022,** *14* (8), 942-948.
(17) Hunt, J. R.; Tseng, C.; Dawlaty, J. M., Donor–acceptor preassociation, excited state solvation threshold, and optical energy cost as challenges in chemical applications of photobases. *Faraday Discuss.* **2019,** *216*, 252-268.
(18) Roy, S.; Ardo, S.; Furche, F., 5-methoxyquinoline photobasicity is mediated by water oxidation. *J. Phys. Chem. A* **2019,** *123* (31), 6645-6651.
(19) Driscoll, E. W.; Hunt, J. R.; Dawlaty, J. M., Photobasicity in Quinolines: Origin and Tunability via the Substituents' Hammett Parameters. *J. Phys. Chem. Lett.* **2016,** *7* (11), 2093-2099.
(20) Driscoll, E. W.; Hunt, J. R.; Dawlaty, J. M., Proton capture dynamics in quinoline photobases: substituent effect and involvement of triplet states. *J. Phys. Chem. A* **2017,** *121* (38), 7099-7107.
(21) Arnaut, L. G.; Formosinho, S. J., Excited-state proton transfer reactions I. Fundamentals and intermolecular reactions. *J. Photochem. Photobiol., A* **1993,** *75* (1), 1-20.
(22) Sheng, W.; Nairat, M.; Pawlaczyk, P. D.; Mroczka, E.; Farris, B.; Pines, E.; Geiger, J. H.; Borhan, B.; Dantus, M., Ultrafast dynamics of a "Super" photobase. *Angew. Chem. Int. Edit.* **2018,** *57* (45), 14742-14746.
(23) Ryan, E. T.; Xiang, T.; Johnston, K. P.; Fox, M. A., Absorption and fluorescence studies of acridine in subcritical and supercritical water. *J. Phys. Chem. A* **1997,** *101* (10), 1827-1835.
(24) Favaro, G.; Mazzucato, U.; Masetti, F., Excited state reactivity of aza aromatics. I. Basicity of 3-styrylpyridines in the first excited singlet state. *J. Phys. Chem.* **1973,** *77* (5), 601-604.

(25) Jiménez-Sánchez, A.; Santillan, R., A photochromic–acidochromic HCl fluorescent probe. An unexpected chloride-directed recognition. *Analyst* **2016,** *141* (13), 4108-4120.
(26) Munitz, N.; Avital, Y.; Pines, D.; Nibbering, E. T. J.; Pines, E., Cation-Enhanced Deprotonation of Water by a Strong Photobase. *Isr. J. Chem.* **2009,** *49* (2), 261-272.
(27) Akulov, K.; Simkovitch, R.; Erez, Y.; Gepshtein, R.; Schwartz, T.; Huppert, D., Acid effect on photobase properties of curcumin. *J. Phys. Chem. A* **2014,** *118* (13), 2470-2479.
(28) Irie, M., Light-induced reversible pH change. *J. Am. Chem. Soc.* **1983,** *105* (7), 2078-2079.
(29) Holmes Jr, E. O., The effect of the properties of solvents of various dielectric constants and structures on the photoionization of the leucocarbinols and leucocyanides of malachite green, crystal violet, and sunset orange and related phenomena. *J. Phys. Chem.* **1966,** *70* (4), 1037-1046.
(30) Abbruzzetti, S.; Carcelli, M.; Pelagatti, P.; Rogolino, D.; Viappiani, C., Photoinduced alkaline pH-jump on the nanosecond time scale. *Chem. Phys. Lett.* **2001,** *344* (3-4), 387-394.
(31) Uda, R. M.; Takenaka, D., Malachite green leuco derivatives as photobase generators for initiating crosslinking and polymerization. *Mater. Lett.* **2021,** *303*, 130541.
(32) Burnstine-Townley, A.; Mondal, S.; Agam, Y.; Nandi, R.; Amdursky, N., Light-Modulated Cationic and Anionic Transport across Protein Biopolymers**. *Angew. Chem. Int. Edit.* **2021,** *60* (46), 24676-24685.
(33) Yucknovsky, A.; Rich, B. B.; Westfried, A.; Pokroy, B.; Amdursky, N., Self-Propulsion of Droplets via Light-Stimuli Rapid Control of Their Surface Tension. *Adv. Mater. Interfaces* **2021,** *8* (22), 2100751.
(34) Demianets, I.; Hunt, J. R.; Dawlaty, J. M.; Williams, T. J., Optical pKa Control in a Bifunctional Iridium Complex. *Organometallics* **2019,** *38* (2), 200-204.
(35) Yucknovsky, A.; Shlosberg, Y.; Adir, N.; Amdursky, N., Photocurrent Generation and Polarity Switching in Electrochemical Cells through Light-induced Excited State Proton Transfer of Photoacids and Photobases. *Angew. Chem.* **2023,** *135* (28), e202301541.
(36) Liu, H.; Xu, Y.; Li, F.; Yang, Y.; Wang, W.; Song, Y.; Liu, D., Light-driven conformational switch of i-motif DNA. *Angew. Chem.* **2007,** *119* (14), 2567-2569.
(37) Irie, M.; Kunwatchakun, D., Photoresponsive polymers. 8. Reversible photostimulated dilation of polyacrylamide gels having triphenylmethane leuco derivatives. *Macromolecules* **1986,** *19* (10), 2476-2480.
(38) Yang, B.; Li, L.; Du, K.; Fan, B.; Long, Y.; Song, K., Photo-responsive photonic crystals for broad wavelength shifts. *Chem. Commun.* **2018,** *54* (24), 3057-3060.
(39) Yucknovsky, A.; Mondal, S.; Burnstine-Townley, A.; Foqara, M.; Amdursky, N., Use of Photoacids and Photobases To Control Dynamic Self-Assembly of Gold Nanoparticles in Aqueous and Nonaqueous Solutions. *Nano Lett.* **2019,** *19* (6), 3804-3810.
(40) Xu, G.; Li, J.; Deng, J.; Yin, L.; Zheng, Z.; Ding, X., A rhythmic assembly system with fireflies' function based on reversible formation of dynamic covalent bonds driven by a pH oscillator. *RSC Adv.* **2015,** *5* (129), 106294-106297.
(41) Shalaby, A. A.; Mohamed, A. A., Determination of acid dissociation constants of Alizarin Red S, Methyl Orange, Bromothymol Blue and Bromophenol Blue using a digital camera. *RSC Adv.* **2020,** *10* (19), 11311-11316.
(42) Fain, V. Y.; Zaitsev, B.; Ryabov, M., Metal complexes with alizarin and alizarin red S: electronic absorption spectra and structure of ligands. *Russ. J. Coord. Chem.* **2004,** *30*, 365-370.
(43) Felix, L. D., Kinetics and thermodynamic study of alkaline fading of Malachine Green in aqueous solution. *Journal of Applied and Fundamental Sciences* **2017,** *3* (2), 52.
(44) Raj, V.; Sarathi, A.; Chandrakala, T.; Dhanalakshmi, S.; Sudha, R.; Rajasekaran, K., Guest-host interactions in the alkaline bleaching of triphenylmethane dyes catalyzed by β-cyclodextrin. *J. Chem. Sci.* **2009,** *121* (4), 529-534.

(45) Abed, O. H.; Isaacs, N. S., Volume profiles for reactions of Malachite Green with anionic nucleophiles. *J. Chem. Soc., Perkin Trans. 2* **1983,** (6), 839-842.
(46) Nandi, R.; Amdursky, N., The Dual Use of the Pyranine (HPTS) Fluorescent Probe: A Ground-State pH Indicator and an Excited-State Proton Transfer Probe. *Acc. Chem. Res.* **2022,** *55* (18), 2728-2739.
(47) Tomsho, J. W.; Benkovic, S. J., Elucidation of the mechanism of the reaction between phenylboronic acid and a model diol, Alizarin Red S. *J. Org. Chem.* **2012,** *77* (5), 2098-2106.